

## Original Article

# miR-638 acts as an oncogene and predicts poor prognosis in renal cell carcinoma

Xiang Pan<sup>2\*</sup>, Tao He<sup>3\*</sup>, Xiqi Peng<sup>1,4\*</sup>, Hang Li<sup>1</sup>, Fangting Zhang<sup>1</sup>, Yongqing Lai<sup>1</sup>

<sup>1</sup>Guangdong and Shenzhen Key Laboratory of Male Reproductive Medicine and Genetics, Peking University Shenzhen Hospital, Shenzhen 518036, Guangdong, P. R. China; <sup>2</sup>Department of Urology, Affiliated Hospital of Yangzhou University, Yangzhou University, Yangzhou 225000, Jiangsu, P. R. China; <sup>3</sup>Department of Urology, Shenzhen People's Hospital (The Second Clinical Medical College, Jinan University; The First Affiliated Hospital, Southern University of Science and Technology), Shenzhen 518020, Guangdong, P. R. China; <sup>4</sup>Shantou University Medical College, Shantou 515041, Guangdong, P. R. China. \*Equal contributors.

Received October 25, 2019; Accepted June 3, 2020; Epub July 15, 2020; Published July 30, 2020

**Abstract:** Objective: The aim of this study was to investigate the function and prognostic value of miR-638 in renal cell carcinoma (RCC). Methods: Expression of miR-638 in RCC tissues and corresponding noncancerous tissues were examined by reverse transcription quantitative polymerase chain reaction (RT-qPCR). To explore the effects of miR-638 on cell migration, invasion, viability, and apoptosis of RCC cells, wound scratch, transwell, MTT, CCK-8, and flow cytometry assays were performed. Kaplan-Meier and Cox regression analyses were used to evaluate the relationship between miR-638 expression and prognosis of RCC patients. Potential target genes of miR-638 were predicted and validated via multiple bioinformatics analyses. Results: miR-638 was upregulated in RCC tissues when compared with corresponding noncancerous tissues ( $P < 0.05$ ). Upregulation of miR-638 expression by transfection with a synthetic miR-638 mimic promoted cell migration, invasion, and viability and suppressed cell apoptosis. Moreover, Kaplan-Meier analysis revealed that upregulation of miR-638 associated with shorter overall survival (OS;  $P = 0.001$ ). Cox univariate and multivariate regression analysis suggested that miR-638 expression is an independent predictive factor for the prognosis of RCC patients ( $P = 0.004$ ). KCNQ1, DNAJC6, and PNP were identified as potential target genes of miR-638. Conclusions: The results of this study demonstrated that miR-638 functions as an oncogene in RCC and has the potential to be a prognostic biomarker for RCC.

**Keywords:** microRNA, miR-638, renal cell carcinoma, oncogene, biomarkers

## Introduction

Renal cell carcinoma (RCC) is a common, malignant, urological tumor that occurs mainly in adults and accounts for ~3% of all malignant tumors in adults [1]. As the third most common cancer of the urological system, RCC has the highest mortality rate [2]. Surgery is the only effective treatment for RCC because it is resistant to both chemotherapy and radiotherapy [3]. Unfortunately, many RCC patients have been misdiagnosed at the early stage, thus ~30% of patients have suffered from metastases at the time of diagnosis and have missed the opportunity for surgical treatment [4]. To overcome this dilemma, there is an urgent need to improve knowledge of RCC, to identify available biomarkers for early diagnosis, and to improve surveillance and targeted therapy.

MicroRNAs (miRNAs) are endogenous, small non-coding RNAs of 19-22 nucleotides that fine-tune expression of protein-coding or non-coding genes [5, 6]. miRNAs have been shown to regulate expression of more than 30% of mRNAs coded by the human genome [6]. Increasing evidence suggests that miRNAs regulate many physiological and pathological conditions, including cancer [7]. In tumorigenesis, miRNAs function as oncogenes and tumor suppressors via their target genes [8]. Current clinical trials suggest that aberrantly expressed miRNAs relate to cancer pathogenesis and drug resistance [9, 10], and studies have shown that miRNAs can function as biomarkers for disease diagnosis, prognosis, and drug efficacy [11].

Previous studies have demonstrated that miR-638 is dysregulated in many human malignan-

**Table 1.** Clinicopathological features of RCC patients

Characteristics	Number of cases
Mean age (range) in years	50 (25-70)
Sex	
Male/Female	14/5
Histological type	
Clear cell/Papillary	16/3
PT-stage	
T1/T2/T3+T4	11/5/3
Fuhrman grade	
I/II/III+IV	13/4/2
AJCC clinical stages	
I/II/III+IV	11/4/4

PT, primary tumor; AJCC, American Joint Committee on Cancer.

cies, such as gastric cancer [12], colorectal carcinoma [13], breast cancer [14], non-small-cell lung cancer [15], and leukemia [16]. However, the clinical significance and function of miR-638 in RCC remains to be verified. Two microarray chip studies showed that miR-638 is upregulated in RCC [17, 18]. In this study, we evaluated miR-638 expression in RCC tissues and cell lines using quantitative real-time polymerase chain reaction (qPCR), and then we explored the function of miR-638 in RCC cell migration, viability, invasion, and apoptosis. In addition, we evaluated the relationship between miR-638 expression and prognosis of RCC patients by Kaplan-Meier analysis and Cox regression analysis. Using multiple bioinformatics analyses, we identified three potential target genes of miR-638 that exhibited strong prognostic values.

## Materials and methods

### Sample collection

Nineteen paired RCC tissues and corresponding noncancerous tissues located 2.5 cm away from visible RCC lesions were collected in Peking University Shenzhen Hospital from 2013-2015 after patients provided informed consent. The RCC patients had not received chemotherapy or radiotherapy prior to tissue sampling. Once dissected, all RCC tissues and corresponding noncancerous tissues were immediately immersed in RNAlater (Qiagen, Hilden, Germany) and stored in liquid nitrogen (-80°C)

for further study. Clinicopathological information for all RCC patients is shown in **Table 1**. The Ethics Committees of Peking University Shenzhen Hospital approved this study.

### Paraffin-embedded RCC specimens

Formalin-fixed paraffin-embedded (FFPE) RCC samples were collected from Peking University Shenzhen Hospital. The clinical stages of all the RCC specimens were determined according to the 2009 American Joint Committee on Cancer (AJCC) staging system. Total RNA was extracted from the FFPE samples using the miRNeasy FFPE kit (Qiagen).

### Cell culture and transfection

Human embryo kidney cell line 293T (293T) and three human RCC cell lines (786-O, ACHN, and Caki-1) were obtained from American Type Culture Collection (ATCC, Manassas, VA, USA). 293T, 786-O and ACHN were grown in Dulbecco's modified Eagle's medium (DMEM; Gibco, Carlsbad, CA, USA) and Caki-1 was grown in McCoy's 5A medium (Gibco, Carlsbad, CA, USA). Media were supplemented with 10% fetal bovine serum (FBS; Gibco, Carlsbad, CA, USA), 1% glutamate (Gibco, Carlsbad, CA, USA), and 1% antibiotics (100 U/ml penicillin, 100 mg/ml streptomycin). Cell cultures were incubated in a humidified atmosphere containing 5% CO<sub>2</sub> at 37°C.

Chemically synthesized miR-638 mimic or inhibitor (GenePharma, Shanghai, China) was transfected into cells using Lipofectamine 2000 (Invitrogen, Carlsbad, CA, USA), which was mixed in Opti-MEM I Reduced Serum Medium (Gibco, Carlsbad, CA, USA). After 24 h of incubation, qRT-PCR was used to test the transfection efficacy of miR-638 mimic or inhibitor into RCC cells. The miR-638 mimic and inhibitor sequences used are shown in **Table 2**.

### Total RNA extraction, cDNA synthesis, and qPCR

Total RNA from tissues and cells was extracted with TRIzol reagent (Invitrogen Life Technologies, Carlsbad, CA, USA) and purified using the RNeasy Maxi kit (Qiagen, Hilden, Germany) according to the manufacturer's instructions. RNA concentration was measured on a NanoDrop 2000/2000c (Thermo, USA). Only RNA

## miR-638 as an oncogene and prognostic biomarker in RCC

**Table 2.** Sequences used in this study

Primer	Sequences
miR-638 forward primer	5'-AGGGATCGCGGGCGGGTGGCGGCCT-3'
miR-638 reverse primer	Universal primer (miScript SYBR Green PCR kit)
miR-638 mimic	Sense: 5'-AGGGAUCGCGGGCGGGUGGCGGCCU-3' Antisense: 5'-GCCGCCACCCGCCCGCAUCCUUU-3'
NC	Sense: 5'-UUCUCCGAACGUGUCACGUTT-3' Antisense: 5'-ACGUGACACGUUCGGAGAATT-3'
miR-638 inhibitor	5'-AGGCCGCCACCCGCCCGCAUCCCU-3'
inhibitor NC	5'-CAGUACUUUUGUGUAGUACAA-3'
U6 forward primer	5'-CTCGCTTCGGCAGCACA-3'
U6 reverse primer	5'-ACGCTTACGAATTTGCGT-3'

NC, negative control.

samples with 260/280 ratios of 1.8-2.1 were used in further experiments. 1 µg total RNA of each sample was reverse transcribed to cDNA using the miScript Reverse Transcription kit (Qiagen, Germany) according to the manufacturer's instructions. The expression level of miR-638 was determined by real-time qPCR (RT-qPCR) using the miScript SYBR Green PCR kit (Qiagen, Germany) and the Roche Lightcycler 480 Real-Time PCR System according to the manufacturer's instructions. U6 expression was used as the internal control. The primer sequences used are shown in **Table 2**. PCR was performed using cDNAs from inhibitor-transfected cells, mimic-transfected cells, inhibitor negative control (NC) cells, and NC cells in triplicate. The PCR protocol was 95°C for 15 min followed by 40 cycles of 94°C for 15 s, 55°C for 30 s, and 72°C for 30 s. Expression levels were analyzed using the  $2^{-\Delta\Delta Ct}$  method [19].

### Wound scratch assay

The wound scratch assay was used to examine the migratory ability of ACHN and 786-O cells *in vitro*. Approximately  $5 \times 10^5$  cells were seeded into each well of a 12-well dish. When cells reached 75-85% confluence, they were transfected with 40 pmol of chemically synthesized miR-638 inhibitor, mimic, inhibitor NC, or NC using Lipofectamine 2000, and incubated for 6 h. Then, a sterile 200 µl pipette tip was used to scratch a clear line through the cell monolayer, cells were rinsed with phosphate-buffered saline (PBS), and cultured in serum-free DMEM in a humidified chamber containing 5% CO<sub>2</sub> at 37°C for another 24 h. Using a digital camera system, we obtained images of the scratches at 0 h and 24 h. The experiments were performed

in triplicate and repeated three or more independent times.

### MTT assay and CCK-8 assay

The 3-(4, 5-dimethylthiazol-2-yl)-2, 5-diphenyltetrazolium bromide (MTT) assay was conducted to examine the effects of miR-638 on 786-O and ACHN cell viability *in vitro*. Approximately 5,000 RCC cells were seeded in each well of a 96-well

plate, transfected with 5 pmol of miR-638 inhibitor, mimic, inhibitor NC, or NC, and incubated for 0, 24, 48, or 72 h. Then, 20 µl of MTT (5 mg/ml, Sigma-Aldrich, St Louis, MO, USA) was added into each well and the plates were incubated at 37°C for 4 h. The reaction was stopped by the addition of 150 µl of dimethylsulfoxide (DMSO, Sigma, Shanghai, China) and agitation for 15 min at room temperature. The optical density (OD) of each well was measured at a wavelength of 490 nm with a microplate reader (Bio-Rad, Hercules, CA, USA).

Viability of 786-O and ACHN cells *in vitro* was examined using Cell Counting Kit-8 (CCK-8, Beyotime Institute of Biotechnology, Shanghai, China) according to the manufacturer's instructions. In each well of a 96-well plate ~5,000 RCC cells were seeded and after 24 h, the cells were transfected with 5 pmol of miR-638 inhibitor, mimic, inhibitor NC, or NC, and incubated for 0, 24, 48, or 72 h. Then, 15 µl of CCK-8 was added into each well, incubated for 3 h, and the OD of each well was measured at a wavelength of 490 nm using a microplate reader (Bio-Rad, Hercules, CA, USA).

### Transwell assay

The transwell assay was performed to assess cell migration and invasion of 786-O and ACHN cells *in vitro*. Transwell chamber inserts (BD, USA) with Matrigel (BD, USA) were used for analysis of invasion and transwell chamber inserts without Matrigel were used for analysis of migration according to the manufacturer's instructions. After transfection with miR-638 inhibitor, mimic, inhibitor NC, or NC, 10,000 RCC cells in 200 µl serum-free medium were

seeded into the upper chambers of the inserts. Medium containing 10% FBS was added to the bottom of the inserts. Cells were allowed to migrate for 40 h and to invade for 60 h. The cells that migrated or invaded to the bottom of the inserts were stained with crystal violet and counted using a microscope. The experiments were performed in triplicate and repeated three or more independent times.

### Flow cytometry

Flow cytometry was used to evaluate the rate of early apoptosis of 786-O and ACHN cells. Approximately  $3 \times 10^5$  RCC cells were seeded into 6-well plates and cultured at 37°C with 5% CO<sub>2</sub> for 24 h. Once the cells reached a confluence of ~70%, they were transfected with 200 pmol of miR-638 inhibitor, mimics, inhibitor NC, or NC. 48 h after transfection, all cells, including floating and adherent cells, were harvested, washed twice with cold PBS, and resuspended in 100 µl 1 × binding buffer. Then, 5 µl of Annexin V and 3 µl of PI (Invitrogen, Carlsbad, CA, USA) were added to each cell suspension, and the mixtures were incubated at room temperature for 15 min, and 400 µl of binding buffer was added to each tube. The samples were then analyzed by flow cytometry (EPICS, XI-4, Beckman, CA, USA) to determine the rate of apoptosis. The experiments were performed in triplicate and repeated three or more independent times.

### Target genes prediction and validation

miRNA-mRNA predictions were made using miRWALK (<http://mirwalk.umm.uni-heidelberg.de>) [20], an online prediction tool. RNA sequencing data from RCC patients were downloaded from The Cancer Genome Atlas (TCGA) database (<https://www.cancergenome.nih.gov>) and the Linear Models for Microarray Data (LIMMA) package in R software (version 3.5.3) was used to identify downregulated genes in cancerous tissue versus corresponding normal tissue with a cut-off criteria of  $|\log_2FC| > 1$  and FDR < 0.05. Genes that were predicted by miRWALK and downregulated were uploaded to the Enrichr database (<https://amp.pharm.mssm.edu/Enrichr/>) [21] for functional annotation and the Search Tool for the Retrieval of Interacting Genes (STRING) database [22] was used to build a protein-protein interaction (PPI) network. Using an App called cytoHubba in Cytoscape

software (version 3.7.1), we calculated the degree of connectivity for each gene and selected the top 20 most central genes in the PPI network. The selected central genes were further validated by Gene expression profiling interactive analysis (GEPIA; <http://gepia.cancer-pku.cn/>), a website for cancer and normal gene expression profiling and interactive analyses.

### Statistical analysis

For comparing expression of miR-638 in matched tumor/normal samples, the paired t-test was used. The relative expression of miR-638 in tissues was presented as mean ± standard error (SE). Other data were presented as the mean ± standard deviation (SD) from three independent experiments. Associations between miR-638 expression and clinical information were evaluated using the Fisher's Exact test or the Pearson chi-square test. Kaplan-Meier analysis combined with the Log-rank test was used for the survival analysis. Cox univariate and multivariate regression analyses were performed to assess relationships between clinical information, miR-638 expression, and survival of RCC patients. All the statistical analyses were carried out with the statistical software package SPSS 20.0 (SPSS Inc. Chicago, IL, USA). Statistical significance was determined using the Student's t-test. *P*-values < 0.05 were considered statistically significant. \**P* < 0.05, \*\**P* < 0.01.

## Results

### miR-638 was upregulated in RCC tissues and cell lines

Expression of miR-638 in 19 RCC tissues and adjacent normal tissues was measured by qPCR, and the relative expression of miR-638 [ $\log_2\text{Ratio (T/N)}$ ] is shown (**Figure 1A** and **1B**). Expression of miR-638 was higher in RCC tissues (mean relative expression = 2.87) than in adjacent normal tissues (*P* < 0.01). Expression of miR-638 was higher in the RCC cell lines 786-O and ACHN than in 293T cells (**Figure 1C**), thus we used 786-O and ACHN cells for additional *in vitro* assays. qRT-PCR was used to evaluate the transfection efficacy of miR-638 into RCC cells. miR-638 expression in 786-O and ACHN was significantly upregulated after transfection with miR-638 mimics while downregulated after transfection with miR-638

## miR-638 as an oncogene and prognostic biomarker in RCC

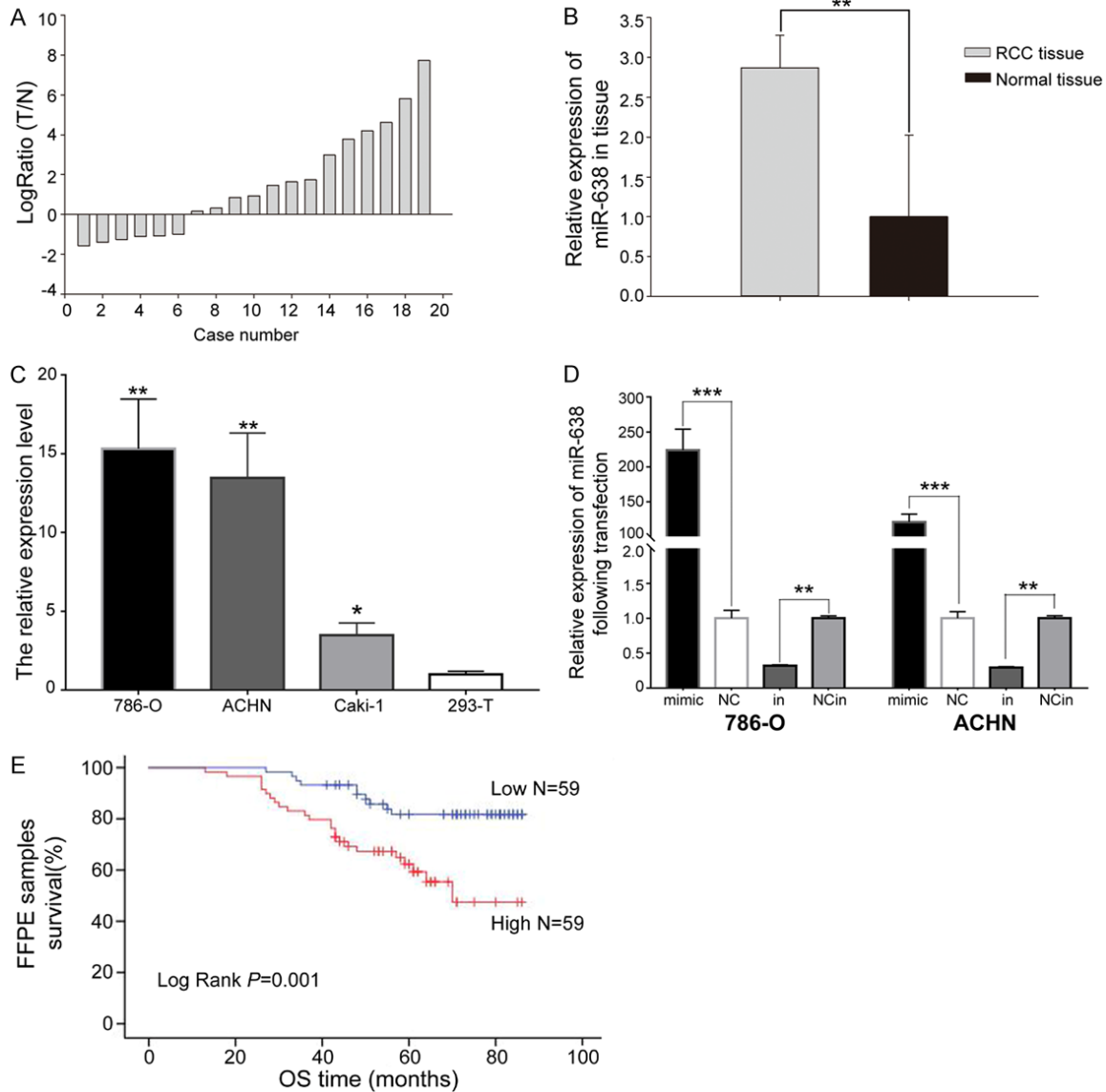


**Figure 1.** miR-638 is upregulated in RCC and correlated with poor prognosis of RCC patients. A. Log<sub>2</sub> Ratios (T/N) of miR-638 expression in 19 paired tissues. T = RCC tissues and N = normal tissues. B. Relative expression of miR-638 was higher in RCC tissues than in normal tissues. C. Relative expression of miR-638 was higher in 786-O, ACHN, and Caki-1 cells than in 293T cells. D. miR-638 expression in 786-O and ACHN cells increased after transfection with the miR-638 mimic and decreased after transfection with the miR-638 inhibitor when compared with the corresponding NC groups. E. RCC patients in the high miR-638 expression group had shorter overall survival (OS) than RCC patients in the low miR-638 expression group. The patients were stratified into high-level and low-level group according to the median cut-off. \* $P < 0.05$ , \*\* $P < 0.01$ , \*\*\* $P < 0.001$ .

inhibitor when compared with that transfected with corresponding negative control (**Figure 1D**).

### *Upregulation of miR-638 correlated with poor prognosis of RCC patients*

The Kaplan-Meier curve of miR-638 expression in RCC patients revealed that high miR-638 expression associates with poor prognosis with

the median as cut-off value (log-rank  $P = 0.001$ ; **Figure 1E**). The Fisher's exact test and the Pearson chi-square test found no relationship between miR-638 expression and clinical information, including gender, age, tumor size, and tumor stage (**Table 3**). Cox regression analysis indicated that high miR-638 expression correlated with poor prognosis of RCC patients (univariate analysis: HR = 3.158, 95% CI = 1.497-6.661,  $P = 0.003$ ; multivariate analysis:

**Table 3.** Associations between the miR-638 expression level<sup>1</sup> and clinical information in FFPE renal cancer samples

Variable	Total	Number of patients (%)		P-value <sup>2</sup>
		high miR-638 expression	low miR-638 expression	
Gender				
Male	77	41 (53.2)	36 (46.8)	0.334
Female	41	18 (43.9)	23 (56.1)	
Age in years				
≤ 60	88	43 (48.9)	45 (51.1)	0.672
> 60	30	16 (53.3)	14 (46.7)	
Tumor size in cm				
≤ 4.0	46	22 (47.8)	24 (52.2)	0.706
> 4.0	72	37 (51.4)	35 (48.6)	
Tumor stage				
I+II	87	43 (49.4)	44 (50.6)	0.834
III+IV	31	16 (51.6)	15 (48.4)	

<sup>1</sup>cut-off point: median. <sup>2</sup>calculated using the Fisher's exact test or the Pearson chi-square test.

HR = 2.937, 95% CI = 1.397-6.177,  $P = 0.004$ ; **Table 4**). These results revealed that high miR-638 expression is an independent risk factor for poor survival in RCC patients.

#### miR-638 promoted RCC cell viability

CCK-8 and MTT assays were performed to measure viability of 786-O and ACHN cells *in vitro*. The CCK-8 assay showed that viability of 786-O cells in the mimic group increased 4.08% ( $P < 0.01$ ), 8.31% ( $P < 0.01$ ), and 15.50% ( $P < 0.01$ ) at 0, 24, 48, and 72 h after transfection, respectively, whereas viability of 786-O cells in the inhibitor group decreased 2.77% ( $P < 0.01$ ), 7.17% ( $P < 0.01$ ), and 11.99% ( $P < 0.01$ ), at 0, 24, 48, and 72 h after transfection, respectively, when compared with 786-O cells transfected with the NC or the inhibitor NC (**Figure 2A**). Similarly, the CCK-8 assay (**Figure 2B**) showed that viability of ACHN cells in the mimic group increased 11.91% ( $P < 0.01$ ), 16.93% ( $P < 0.01$ ), and 21.38% ( $P < 0.01$ ) at 0, 24, 48, and 72 h after transfection, respectively, whereas viability of ACHN cells in the inhibitor group decreased 10.49% ( $P < 0.01$ ), 15.99% ( $P < 0.01$ ), and 22.77% ( $P < 0.01$ ) at 0, 24, 48, and 72 h after transfection, respectively, when compared with ACHN cells transfected with the NC or the inhibitor NC.

The MTT assay showed that viability of 786-O cells in the mimic group increased 9.17% ( $P <$

0.05), 19.22% ( $P < 0.05$ ), and 33.88% ( $P < 0.01$ ) at 24, 48, and 72 h after transfection, respectively, whereas 786-O cells in the inhibitor group decreased 9.31% ( $P < 0.05$ ), 16.48% ( $P < 0.01$ ), and 25.46% ( $P < 0.01$ ) at 24, 48, and 72 h after transfection, respectively, when compared with 786-O cells transfected with NC or inhibitor NC (**Figure 2C**). Similarly, the MTT assay showed that viability of ACHN cells in the mimic group increased 9.71% ( $P < 0.01$ ), 21.74% ( $P < 0.01$ ), and 36.37% ( $P < 0.001$ ) at 24, 48, and 72 h after transfection, respectively, whereas viability of ACHN cells in the inhibitor group decreased 9.55% ( $P < 0.01$ ), 14.80% ( $P < 0.01$ ), and 26.33% ( $P < 0.01$ ) at 24, 48, and 72 h after transfection, respectively, when compared with ACHN cells transfected with the NC or the inhibitor NC (**Figure 2D**).

#### miR-638 promoted RCC cell migration

The wound scratch and transwell assays were conducted to evaluate the migratory ability of ACHN and 786-O cells *in vitro*. Upon transfection of ACHN cells with the miR-638 mimic for 24 h, the distance of ACHN cell migration increased 68.44% ( $P < 0.01$ ) when compared with ACHN cells transfected with the NC (**Figure 3A**). In contrast, in ACHN cells transfected with the miR-638 inhibitor, the distance of cell migration decreased 42.08% ( $P < 0.01$ ) when compared with ACHN cells transfected with the inhibitor NC (**Figure 3A**).

Similarly, in 786-O cells transfected with the miR-638 mimic for 24 h, the distance of cell migration increased 25.56% ( $P < 0.01$ ) when compared with 786-O cells transfected with the NC (**Figure 3B**). In contrast, in 786-O cells transfected with the miR-638 inhibitor, the distance of cell migration decreased 26.10% ( $P < 0.01$ ) when compared with 786-O cells transfected with the inhibitor NC (**Figure 3B**).

The transwell assay showed that the migratory ability of ACHN cells increased 58.02% ( $P < 0.01$ ) upon transfection with the miR-638 mimic and decreased 38.73% ( $P < 0.01$ ) upon transfection with the miR-638 inhibitor when compared with the NC and inhibitor NC groups, respectively (**Figure 3C**). The migratory ability of 786-O cells increased 24.96% ( $P < 0.01$ ) upon

**Table 4.** The miR-638 expression level and RCC patient survival

Variable	Univariate analysis		Multivariate analysis	
	HR (95% CI)	P-value	HR (95% CI)	P-value
Gender (Male vs Female)	0.790 (0.378-1.652)	0.531		
Age in years (> 60 vs ≤ 60)	1.156 (0.523-2.556)	0.719		
Tumor size in cm (> 4.0 vs ≤ 4.0)	0.965 (0.482-1.929)	0.919		
Tumor stage (I+II vs III+IV)	0.061 (0.027-0.138)	0.000	0.065 (0.029-0.146)	0.000
miR-638 (high vs low)	3.158 (1.497-6.661)	0.003	2.937 (1.397-6.177)	0.004

HR, hazard ratio; 95% CI, 95% confidence interval.

transfection with the miR-638 mimic and decreased 41.96% ( $P < 0.01$ ) upon transfection with the miR-638 inhibitor (**Figure 3D**) when compared with the NC and the inhibitor NC groups, respectively. The results of the wound scratch and transwell assays revealed that miR-638 promotes migration of RCC cells.

#### *miR-638 promoted RCC cell invasion*

The transwell assay was also performed to assess the cell invasion ability of ACHN and 786-O cells *in vitro*. In ACHN cells, invasion increased 69.37% ( $P < 0.01$ ) upon transfection with the miR-638 mimic when compared with cells transfected with the NC (**Figure 3E**). In contrast, ACHN cell invasion decreased 45.99% ( $P < 0.01$ ) upon transfection with the miR-638 inhibitor was when compared with cells transfected with the inhibitor NC (**Figure 3E**). In 786-O cells, invasion increased 30.31% ( $P < 0.01$ ) upon transfection with the miR-638 mimic and decreased 44.16% ( $P < 0.01$ ) upon transfection with the miR-638 inhibitor (**Figure 3F**) when compared with cells transfected with the NC or the inhibitor NC, respectively. The results of the transwell assay demonstrated that miR-638 promotes invasion of RCC cells.

#### *miR-638 suppressed RCC cell apoptosis*

Flow cytometry was performed to evaluate the rate of early apoptosis of ACHN and 786-O cells. The apoptotic rates of ACHN cells transfected with the miR-638 mimic and the NC were 4.87% and 10.29% ( $P < 0.01$ ), respectively (**Figure 4A**). The apoptotic rates of ACHN cells transfected with the miR-638 inhibitor and the inhibitor NC were 13.28% and 9.09% ( $P < 0.01$ ), respectively (**Figure 4B**). The apoptotic rates of 786-O cells transfected with the miR-638 mimic and with the NC were 6.57% and 10.70% ( $P < 0.01$ ), respectively (**Figure 4C**). The apop-

otic rates of 786-O cells transfected with miR-638 inhibitor and the inhibitor NC were 15.66% and 9.47% ( $P < 0.01$ ), respectively (**Figure 4D**). These results showed that miR-638 suppresses RCC cell apoptosis.

#### *Potential target genes of miR-638*

By identifying predicted target genes of miR-638 in miRWALK that were also downregulated in cancerous tissues according to TCGA, we found 193 candidate target genes (**Figure 5A** and **5B**). To determine the potential mechanisms that these genes are involved in, functional enrichment analysis was conducted via an Enrichr database (**Figure 5C-F**). The top 10 enriched gene ontology (GO) terms of biological processes (BPs) were ion transmembrane transport, ion transport, positive regulation of signal transduction, transmembrane transport, positive regulation of epithelial cell migration, positive regulation of transport, heart contraction, brown fat cell differentiation, phagosome acidification, response to epinephrine, cellular response to epinephrine stimulus, and positive regulation of non-canonical WNT signaling pathway (**Figure 5C**). The results of cellular components (CCs) revealed that these genes were mainly enriched in the aggresome, lytic vacuole, actin filament, filopodium, perinuclear region of the cytoplasm, sarcoplasmic reticulum, sarcoplasm, and the integral component of the plasma membrane (**Figure 5D**). The top 10 enriched GO terms of molecular functions (MFs) were acetylcholine receptor binding, voltage-gated potassium channel activity involved in ventricular cardiac muscle cell action potential repolarization, amide transmembrane transporter activity, voltage-gated potassium channel activity involved in cardiac muscle cell action potential repolarization, water transmembrane transporter activity, protein kinase A catalytic subunit binding, water channel activity,

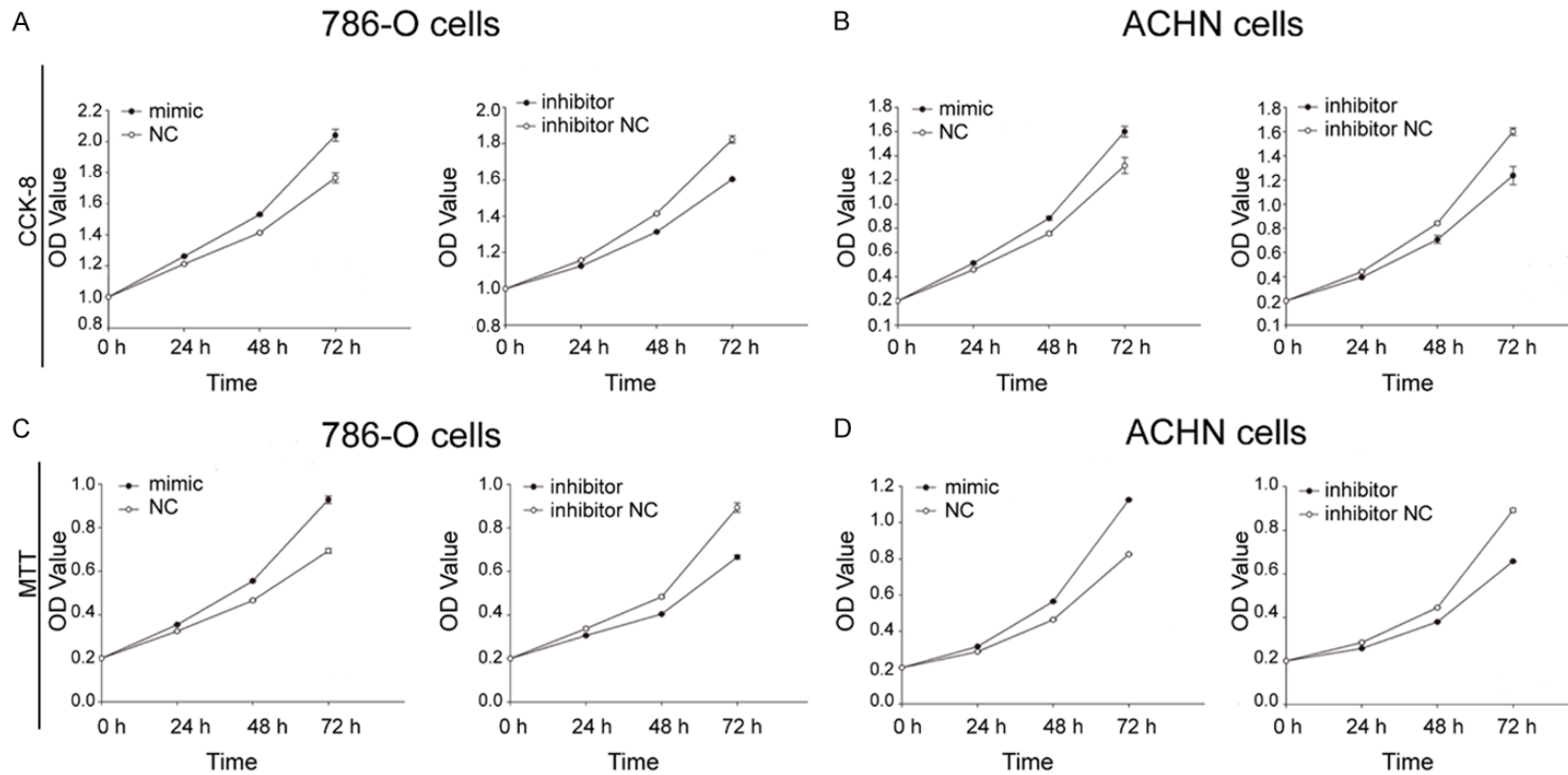


**Figure 2.** The CCK-8 assay (A, B) and the MTT assay (C, D) showed that viability of 786-O and ACHN cells increased after transfection with the miR-638 mimic and decreased after transfection with the miR-638 inhibitor when compared with the corresponding NC groups.

## miR-638 as an oncogene and prognostic biomarker in RCC

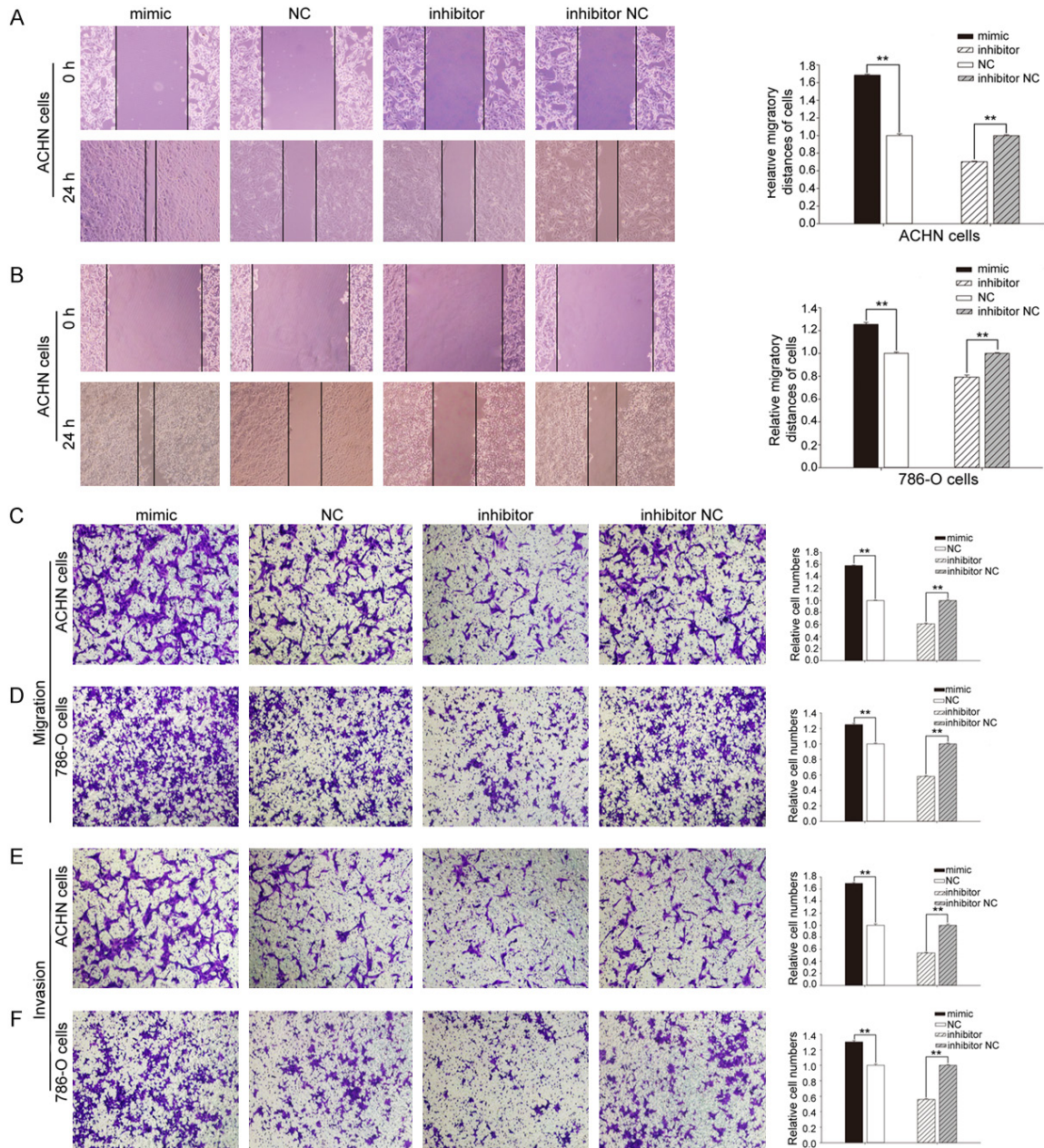


**Figure 3.** miR-638 promotes RCC cells migration and invasion. The wound scratch assay with ACHN cells (A) and 786-O cells (B). Distances of ACHN and 786-O cell migration after transfection with the miR-638 mimic, NC, miR-638 inhibitor, and inhibitor NC showed that upregulation of miR-638 promotes cell migration and downregulation of miR-638 inhibits cell migration. Transwell assays showed that migration of ACHN and 786-O cells increased after transfection with the miR-638 mimic (C, D) and that invasion of ACHN and 786-O cells increased after transfection with the miR-638 mimic (E, F).  $^{**}P < 0.01$ .

voltage-gated cation channel activity, acetylcholine receptor activity, and calcium ion binding (Figure 5E). As for the Kyoto Encyclopedia of Genes and Genomes (KEGG) pathway analysis, the genes were mostly enriched in pathways involving *Vibrio cholerae* infection, collecting

duct acid secretion, epithelial cell signaling in *Helicobacter pylori* infection, calcium signaling, adrenergic signaling in cardiomyocytes, retinol metabolism, gastric acid secretion, synaptic vesicle cycle, Ras signaling, and protein digestion and absorption (Figure 5F).

## miR-638 as an oncogene and prognostic biomarker in RCC

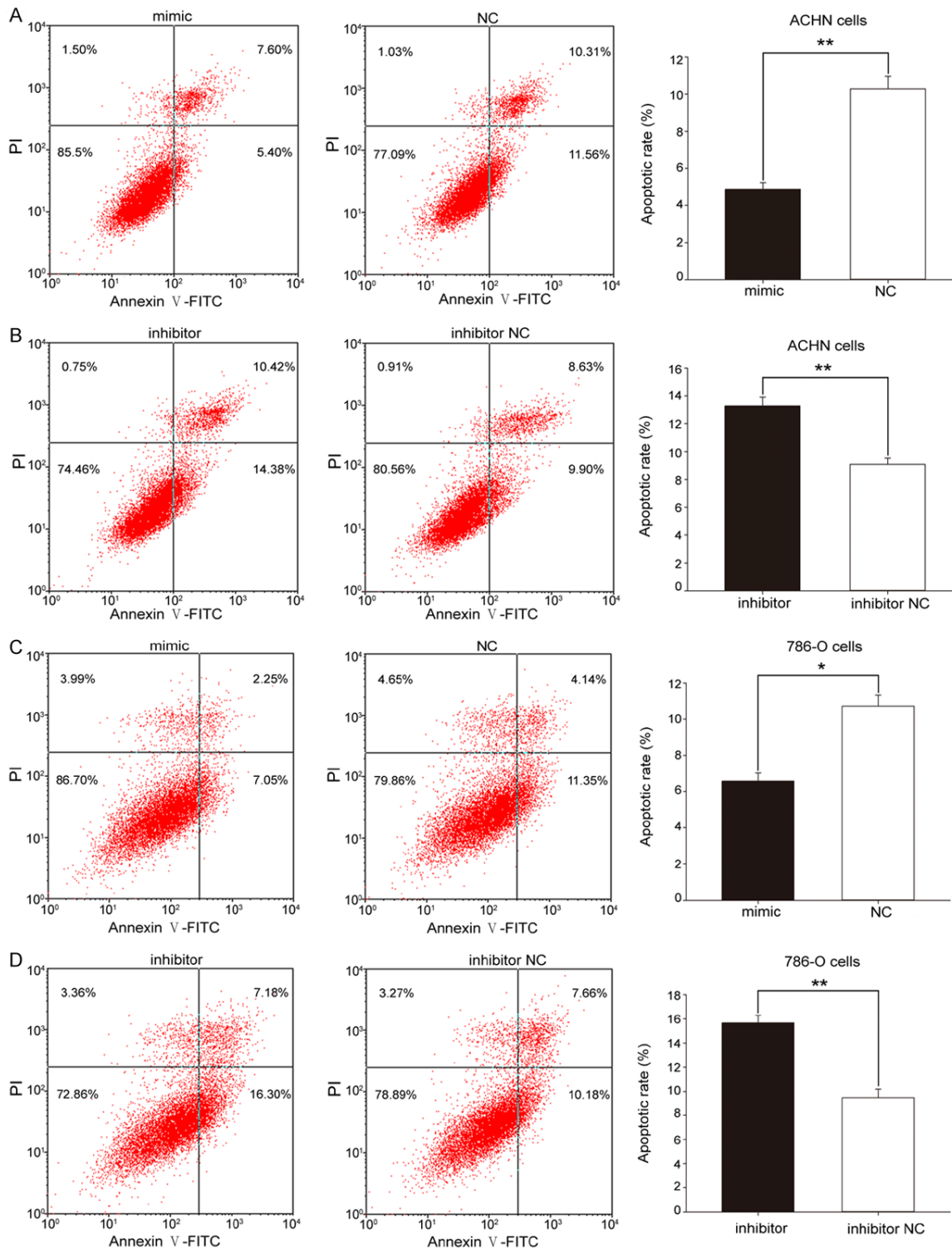
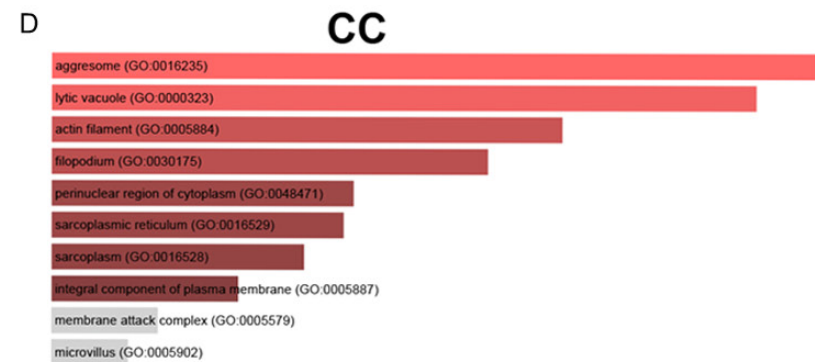
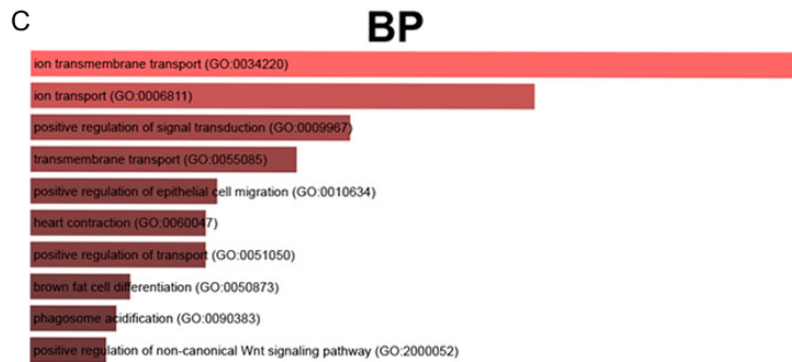
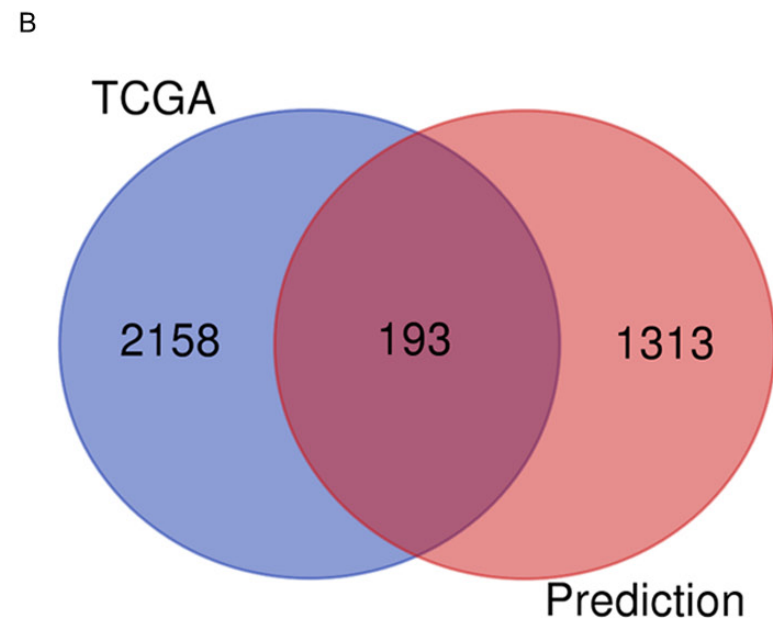
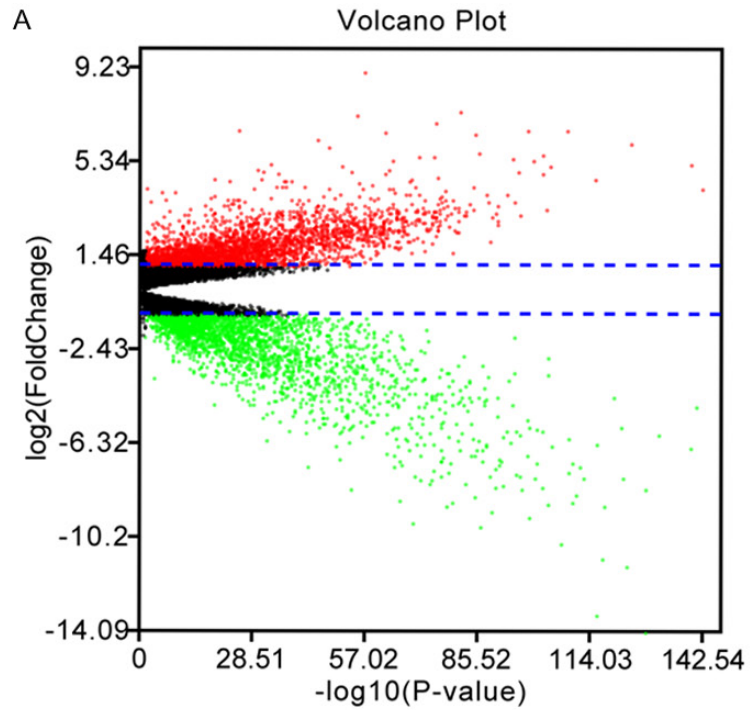


**Figure 4.** miR-638 suppressed ACHN and 786-O cell apoptosis. A. Overexpression of miR-638 as a result of transfection with the miR-638 mimic inhibited ACHN cell apoptosis. B. Downregulation of miR-638 as a result of transfection with the miR-638 inhibitor induced ACHN cell apoptosis. C. Overexpression of miR-638 as a result of transfection with the miR-638 mimic inhibited 786-O cell apoptosis. D. Downregulation of miR-638 as a result of transfection with the miR-638 inhibitor induced 786-O cell apoptosis. \* $P < 0.05$ , \*\* $P < 0.01$ .

After constructing a PPI network with these candidate genes, we used cytoHubba to iden-

tify the top 20 most central genes of the network: AQP4, ATP2B3, PRKCA, CALB1, KCNQ1,

miR-638 as an oncogene and prognostic biomarker in RCC



miR-638 as an oncogene and prognostic biomarker in RCC

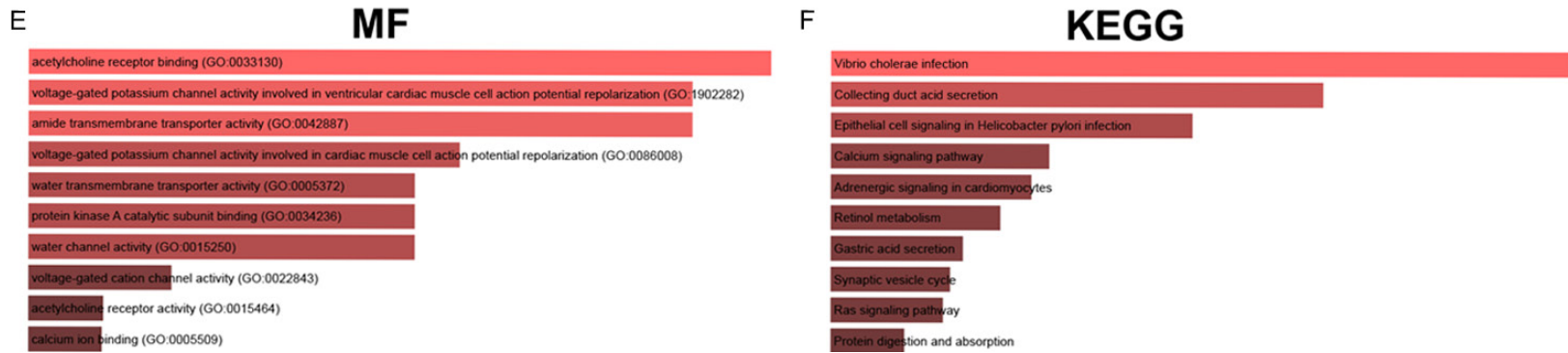
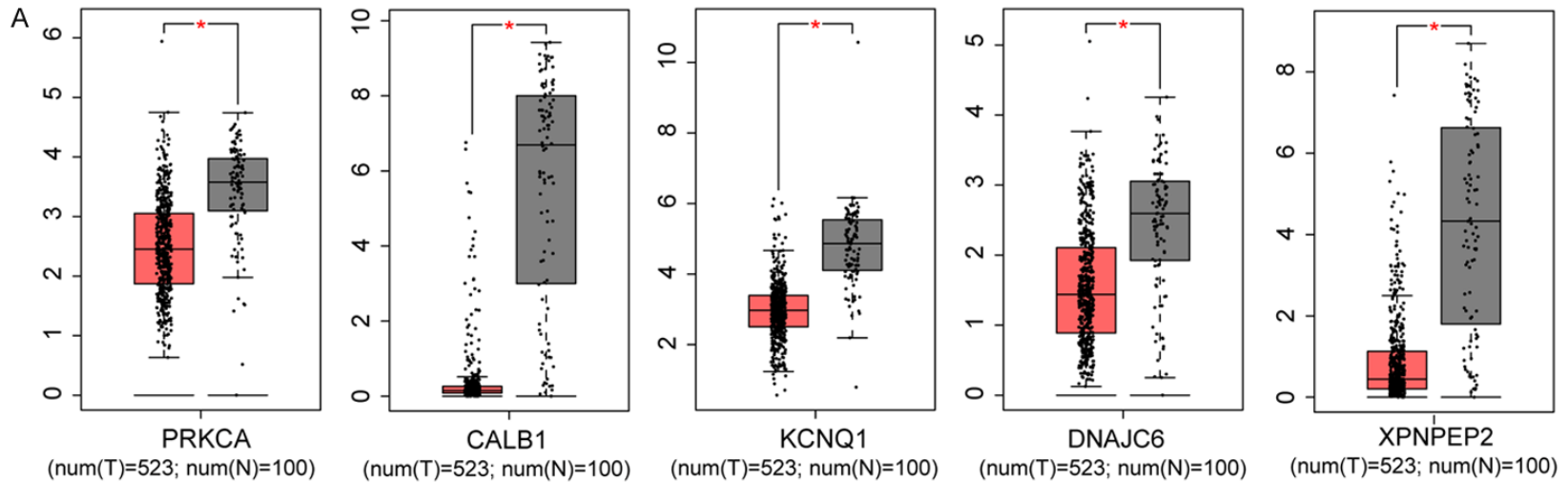


**Figure 5.** Screening potential miR-638 target genes. (A) Differentially expressed genes in RCC from the TCGA database. Red represents upregulated genes and green represents downregulated genes. (B) Venn diagram showing the overlap of genes downregulated in RCC from the TCGA database and genes predicted using the miRWALK database. (C-E) Functional enrichment analysis of the candidate target genes of miR-638. The top 10 most enriched terms in the (C) biological process, (D) cellular component, (E) molecular function, and (F) KEGG pathway analyses are shown.



miR-638 as an oncogene and prognostic biomarker in RCC

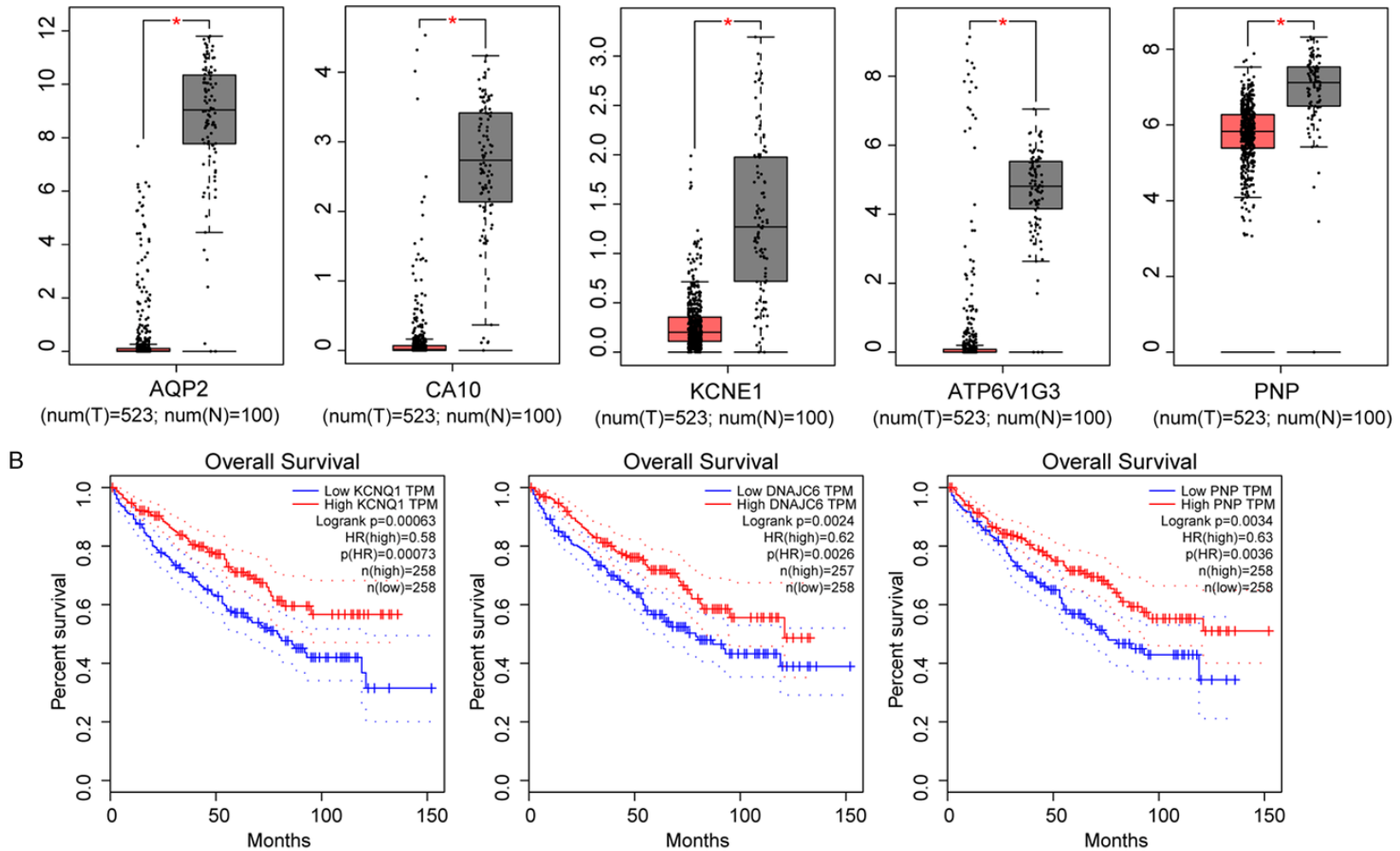


**Figure 6.** Identification of potential miR-638 target genes. A. Ten significantly downregulated candidate target genes of miR-638 were identified among the top 20 most central genes in PPI network. B. Kaplan-Meier curves of potential miR-638 target genes in RCC. The patients were stratified into high-level and low-level group according to the median cut-off. Low expression of KCNQ1, DNAJC6, PNP was correlated with poorer OS of RCC patients. PPI network, protein-protein interaction network; HR, hazard ratio.

ATP6V1G2, SCN2B, DNAJC6, XPNPEP2, CHRNA4, AQP2, DGKB, SLC24A2, CADM2, TRDN, CA10, SNCA, KCNE1, ATP6V1G3, and PNP. GEPIA database results revealed that expression of PRKCA, CALB1, KCNQ1, DNAJC6, XPNPEP2, AQP2, CA10, KCNE1, ATP6V1G3, and PNP were significantly lower in RCC than in normal tissues (**Figure 6A**). Further, Kaplan-Meier analysis indicated that low expression of KCNQ1 ( $P = 0.00063$ ), DNAJC6 ( $P = 0.0024$ ), and PNP ( $P = 0.0034$ ) associated with poor survival of RCC patients with median as the cut-off value (**Figure 6B**). Thus, KCNQ1, DNAJC6, and PNP could be target genes of miR-638.

### Discussion

In this study, we demonstrated that miR-638 was significantly upregulated in RCC tissues and cell lines when compared with corresponding noncancerous tissues and a normal human kidney cell line. And miR-638 could act as a prognostic biomarker in RCC. The results of functional studies *in vitro* suggest that miR-638 acts as an oncogene in RCC. Moreover, using several bioinformatics analyses, we identified KCNQ1, DNAJC6, and PNP as three potential target genes of miR-638 that were significantly downregulated in RCC and negatively associated with survival of RCC patients.

Previous studies demonstrated that miR-638 is dysregulated in many human malignant tumors. Zhao *et al* showed that miR-638 overexpression suppressed cell proliferation in gastric cancer (GC) by targeting the 3'-UTR of specificity protein 2 (SP2) mRNA [12]. Zhang *et al* also showed that miR-638 suppressed cell proliferation in human GC by targeting phospholipase D1 [23]. Moreover, miR-638 has been shown to be downregulated and to act as a tumor suppressor in colorectal carcinoma. miR-638 inhibited cell proliferation, invasion, and cell cycle progression of colorectal carcinoma by targeting TSPAN1 directly [13]. Yang *et al* showed that downregulation of miR-638 in non-small-cell lung carcinoma (NSCLC) promoted cell proliferation and invasion via regulation of SOX2 and induced the epithelial-to-mesenchymal transition (EMT) [15]. It has also been demonstrated that miR-638 affects DNA repair [24, 25]. In some terminally differentiated cells, miR-638 overexpression suppressed DNA damage repair processes by targeting SMC1A

expression [25]. In another study, treatment with miR-638 enhanced sensitivity of triple-negative breast cancer cells to radiation and chemotherapy by regulating BRCA1 expression via a DNA repair pathway [24]. These discoveries indicate that miR-638 plays a role in DNA repair during tumorigenesis. However, the miR-638-mediated molecular pathways that affect cell migration, viability, and apoptosis in RCC remain to be validated by further research.

This study demonstrated that miR-638 acts as an oncogene in RCC by promoting migration, promoting viability, and suppressing apoptosis of RCC cells. In addition, upregulation of miR-638 was shown to be an independent predictive factor for survival of RCC patients. miR-638 has potential as a biomarker for early RCC diagnosis, as a predictor of RCC prognosis, and as a targeted therapeutic for RCC in the future.

### Acknowledgements

Yongqing Lai and Fangting Zhang designed the experiments. Xiang Pan, Tao He, and Xiqi Peng performed the experiments, analyzed and interpreted the data. Tao He and Xiqi Peng were major contributors in writing the manuscript. The final version of the manuscript has been read and approved by all authors, and each author believes that the manuscript represents honest work. This study was supported by Basic Research Project of Peking University Shenzhen Hospital (JCYJ2017001, JCYJ2017-004, JCYJ2017005, JCYJ2017006, JCYJ20170-07, JCYJ2017012), Clinical Research Project of Peking University Shenzhen Hospital (LCYJ20-17001), Science and Technology Development Fund Project of Shenzhen (No. JCYJ2018050-7183102747) and Clinical Research Project of Shenzhen Health Commission (No. SZLY2018-023).

### Disclosure of conflict of interest

None.

**Address correspondence to:** Drs. Yongqing Lai and Fangting Zhang, Guangdong and Shenzhen Key Laboratory of Male Reproductive Medicine and Genetics, Peking University Shenzhen Hospital, Shenzhen 518036, Guangdong, P. R. China. Tel: +86-0755-83923333-2731; E-mail: yqlord@outlook.com (YQL); fangtingzhang@126.com (FTZ)

## References

- [1] Siegel RL, Miller KD and Jemal A. Cancer statistics, 2016. *CA Cancer J Clin* 2016; 66: 7-30.
- [2] Patel C, Ahmed A and Ellsworth P. Renal cell carcinoma: a reappraisal. *Urol Nurs* 2012; 32: 182-190; quiz 191.
- [3] Escudier B, Porta C, Schmidinger M, Rioux-Leclercq N, Bex A, Khoo V, Gruenvald V and Horwich A. Renal cell carcinoma: ESMO clinical practice guidelines for diagnosis, treatment and follow-up. *Ann Oncol* 2016; 27: v58-v68.
- [4] Khella HW, Scorilas A, Mozes R, Mirham L, Li-anidou E, Krylov SN, Lee JY, Ordon M, Stewart R, Jewett MA and Yousef GM. Low expression of miR-126 is a prognostic marker for metastatic clear cell renal cell carcinoma. *Am J Pathol* 2015; 185: 693-703.
- [5] Goto Y, Kurozumi A, Enokida H, Ichikawa T and Seki N. Functional significance of aberrantly expressed microRNAs in prostate cancer. *Int J Urol* 2015; 22: 242-252.
- [6] Bartel DP. MicroRNAs: target recognition and regulatory functions. *Cell* 2009; 136: 215-233.
- [7] Esquela-Kerscher A and Slack FJ. Oncomirs - microRNAs with a role in cancer. *Nat Rev Cancer* 2006; 6: 259-269.
- [8] Fendler A, Stephan C, Yousef GM and Jung K. MicroRNAs as regulators of signal transduction in urological tumors. *Clin Chem* 2011; 57: 954-968.
- [9] Garzon R, Calin GA and Croce CM. MicroRNAs in cancer. *Annu Rev Med* 2009; 60: 167-179.
- [10] Tay Y, Rinn J and Pandolfi PP. The multilayered complexity of ceRNA crosstalk and competition. *Nature* 2014; 505: 344-352.
- [11] Hayes J, Peruzzi PP and Lawler S. MicroRNAs in cancer: biomarkers, functions and therapy. *Trends Mol Med* 2014; 20: 460-469.
- [12] Zhao LY, Yao Y, Han J, Yang J, Wang XF, Tong DD, Song TS, Huang C and Shao Y. miR-638 suppresses cell proliferation in gastric cancer by targeting Sp2. *Dig Dis Sci* 2014; 59: 1743-1753.
- [13] Zhang J, Fei B, Wang Q, Song M, Yin Y, Zhang B, Ni S, Guo W, Bian Z, Quan C, Liu Z, Wang Y, Yu J, Du X, Hua D and Huang Z. MicroRNA-638 inhibits cell proliferation, invasion and regulates cell cycle by targeting tetraspanin 1 in human colorectal carcinoma. *Oncotarget* 2014; 5: 12083-12096.
- [14] Zavala V, Perez-Moreno E, Tapia T, Camus M and Carvallo P. miR-146a and miR-638 in BRCA1-deficient triple negative breast cancer tumors, as potential biomarkers for improved overall survival. *Cancer Biomark* 2016; 16: 99-107.
- [15] Xia Y, Wu Y, Liu B, Wang P and Chen Y. Down-regulation of miR-638 promotes invasion and proliferation by regulating SOX2 and induces EMT in NSCLC. *FEBS Lett* 2014; 588: 2238-2245.
- [16] Tanaka M, Oikawa K, Takanashi M, Kudo M, Ohyashiki J, Ohyashiki K and Kuroda M. Down-regulation of miR-92 in human plasma is a novel marker for acute leukemia patients. *PLoS One* 2009; 4: e5532.
- [17] Yi Z, Fu Y, Zhao S, Zhang X and Ma C. Differential expression of miRNA patterns in renal cell carcinoma and nontumorous tissues. *J Cancer Res Clin Oncol* 2010; 136: 855-862.
- [18] Zaravinos A, Lambrou GI, Mourmouras N, Kafatygiotis P, Papagregoriou G, Giannikou K, Delakas D and Deltas C. New miRNA profiles accurately distinguish renal cell carcinomas and upper tract urothelial carcinomas from the normal kidney. *PLoS One* 2014; 9: e91646.
- [19] Livak KJ and Schmittgen TD. Analysis of relative gene expression data using real-time quantitative PCR and the 2(-Delta Delta C(T)) Method. *Methods* 2001; 25: 402-408.
- [20] Sticht C, De La Torre C, Parveen A and Gretz N. miRWalk: an online resource for prediction of microRNA binding sites. *PLoS One* 2018; 13: e0206239.
- [21] Kuleshov MV, Jones MR, Rouillard AD, Fernandez NF, Duan Q, Wang Z, Koplev S, Jenkins SL, Jagodnik KM, Lachmann A, McDermott MG, Monteiro CD, Gundersen GW and Ma'ayan A. Enrichr: a comprehensive gene set enrichment analysis web server 2016 update. *Nucleic Acids Res* 2016; 44: W90-97.
- [22] Szklarczyk D, Gable AL, Lyon D, Junge A, Wyder S, Huerta-Cepas J, Simonovic M, Doncheva NT, Morris JH, Bork P, Jensen LJ and Mering CV. STRING v11: protein-protein association networks with increased coverage, supporting functional discovery in genome-wide experimental datasets. *Nucleic Acids Res* 2019; 47: D607-D613.
- [23] Zhang J, Bian Z, Zhou J, Song M, Liu Z, Feng Y, Zhe L, Zhang B, Yin Y and Huang Z. MicroRNA-638 inhibits cell proliferation by targeting phospholipase D1 in human gastric carcinoma. *Protein Cell* 2015; 6: 680-688.
- [24] Tan X, Peng J, Fu Y, An S, Rezaei K, Tabbara S, Teal CB, Man YG, Brem RF and Fu SW. miR-638 mediated regulation of BRCA1 affects DNA repair and sensitivity to UV and cisplatin in triple-negative breast cancer. *Breast Cancer Res* 2014; 16: 435.
- [25] He M, Lin Y, Tang Y, Liu Y, Zhou W, Li C, Sun G and Guo M. miR-638 suppresses DNA damage repair by targeting SMC1A expression in terminally differentiated cells. *Aging (Albany NY)* 2016; 8: 1442-1456.